Influence of the support crystal structure of WO₃/Au catalysts in CO oxidation

Tamás Firkala[1,2], Balázs Fórizs[1], Eszter Drotár[2], András Tompos[2], Attila L. Tóth[3], Katalin Varga-Josepovits[4], Krisztina László[5], Markku Leskelä[6], Imre Miklós Szilágyi[1,6,7*]

[1]Department of Inorganic and Analytical Chemistry, Budapest University of Technology and Economics, H-1111 Budapest, Szt. Gellért tér 4. Hungary;

[2]Institute of Materials and Environmental Chemistry, Research Centre of Natural Sciences, Hungarian Academy of Sciences, H–1025 Budapest, Pusztaszeri út 59–67. Hungary

[3]Institute for Technical Physics and Materials Science, Research Centre of Natural Sciences, Hungarian Academy of Sciences, H–1121 Konkoly–Thege út 29–33. Budapest, Hungary;

[4]Department of Atomic Physics, Budapest University of Technology and Economics, H–1111 Budapest, Budafoki út 8. Hungary;

[5]Department of Physical Chemistry and Materials Science, Budapest University of Technology and Economics, P.O. Box 92, H–1521 Budapest, Hungary;

[6]Department of Chemistry, University of Helsinki, A.I. Virtasen aukio 1, Helsinki, FI-00550, Finland;

[7]Technical Analytical Chemistry Research Group of the Hungarian Academy of Sciences, Budapest University of Technology and Economics, H-1111 Budapest, Szt. Gellért tér 4., Hungary

*Corresponding author: imre.szilagyi@mail.bme.hu

Abstract

1

Gold nanoparticles (partially below 5 nm in diameter) were successfully deposited on hexagonal and monoclinic WO_3 supports by deposition–precipitation, which had been considered previously not feasible owing to the low isoelectronic point of WO_3. The catalysts were characterized by TEM, SEM, N_2-adsorption, XRD, and XPS. In CO oxidation m-WO_3/Au showed better catalytic activity over 100 °C than h-WO_3/Au. This was explained by that m-WO_3 had higher surface OH coverage, resulting in larger Au nanoparticle loading and thus better catalytic activity.

Graphical abstract
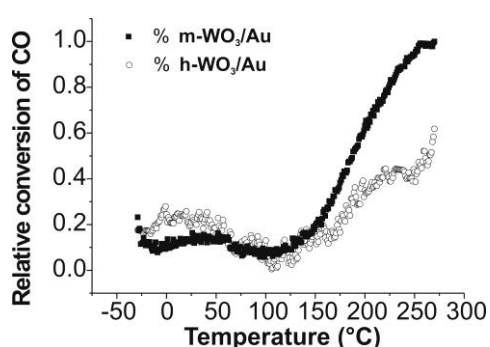
Keywords

WO_3, Au, CO oxidation, catalysis, structure, composition, support

Introduction

Heterogeneous gold catalysts are intensively investigated, as the outstanding catalytic activity of this metal in nanosize has been proven in a lot of reactions and under various

circumstances [1]. It is well known that the activity of gold catalysts highly depends on the gold nanoparticle size, the properties of the support material [2], the preparation process [3], the conditions of the pretreatment [4] etc. Oxidation reactions (e.g. oxidation of alcohols [5], alkenes [6], monosaccharides [7] and carbon monoxide [8]) are good examples for the very high activity of gold catalysts.

The oxidation circumstances of CO by Au nanoparticles have garnered a lot of attention recently [9-11]. CO is a toxic gas, which can irreversibly bond to hemoglobin in human blood, converting it to carboxyhemoglobin, if the concentration of CO approaches 100 ppm in the atmosphere [12].

Semiconductor oxides (TiO_2, WO_3, SnO_2, ZnO, V_2O_5, etc.), which are widely studied as heterogeneous catalysts [13], can be supports for catalytic Au nanoparticles as well [14-16]. Tungsten oxide (WO_3) is a well-known catalyst (e.g. for the selective oxidation of olefins or sulfides [17], reforming reactions [18], etc.), and the application of WO_3 supported noble metal (Pt, Pd) catalysts in CO oxidation is well known [19]. Nevertheless, to the best of our knowledge, the investigation of a WO_3/Au catalyst in CO oxidation has been reported only in one study [20].

Immobilizing gold nanoparticles on WO_3 surfaces was done mainly by physical methods (e.g. by sputtering [20]). The otherwise widely used deposition-precipitation of Au was considered to be impossible on WO_3 previously, due to the low isoelectronic point of WO_3 [21].

Recently a new way has been developed to deposit Au nanoparticles through deposition-precipitation, but it has been used only on Al_2O_3 and SiO_2 supports [22-23]. It was unclear whether this method can be used also on an oxide with low isoelectronic point (i.e. WO_3).

WO$_3$ has different crystalline modifications (e.g. monoclinic, hexagonal [24]). Recently, it was revealed that the hexagonal (h-) and monoclinic (m-) forms of WO$_3$ behaved quite differently in gas sensing [25-30] and photocatalysis [31]. However, it was unclear how they would influence in general the catalytic activity of WO$_3$, and in particular how they would affect catalysis when they are used as supports for Au nanoparticles.

Therefore, we aimed to prepare WO$_3$/Au catalysts and demonstrate that Au nanoparticles can be deposited on WO$_3$ from solution by the deposition-precipitation method. In addition, we explored the activity of WO$_3$/Au catalysts in CO oxidation, and also investigated the influence of the crystal structure (monoclinic or hexagonal) of the WO$_3$ support on catalysis. Recently a new way was developed to prepare h-WO$_3$ and m-WO$_3$ by annealing (NH$_4$)$_x$WO$_{3-y}$ [27], which enabled preparing them with very similar morphologies. This ensured that mostly the different WO$_3$ crystal structures could have effect on catalysis, while the morphologies influenced it to a smaller extent.

Therefore, in this paper we report on the different catalytic activity of m-WO$_3$/Au and h-WO$_3$/Au composites. Gold nanoparticles were synthesized on m-WO$_3$ and h-WO$_3$ with deposition–precipitation (reducing HAuCl$_4$ solution) and consecutive pretreatment (annealing in air at 350 °C). Transmission electron microscopy (TEM), scanning electron microscopy (SEM), low temperature nitrogen adsorption measurement, X-ray diffraction (XRD) and X-ray photoelectron spectroscopy (XPS) were used to characterize the catalysts. The catalytic activity of the composites was tested in CO oxidation.

Experimental

Preparation of Au/WO$_3$ catalysts

Preparing m-WO$_3$ and h-WO$_3$ supports. Hexagonal WO$_3$ and monoclinic WO$_3$ samples were prepared by annealing hexagonal ammonium tungsten bronze, $(NH_4)_{0.33-x}WO_{3-y}$ in air at 470 °C and 600 °C, respectively [25]. The precursor $(NH_4)_{0.33-x}WO_{3-y}$ was obtained by the partial reduction of ammonium paratungstate tetrahydrate (APT), $(NH_4)_{10}[H_2W_{12}O_{42}]\cdot4H_2O$, in H$_2$ at 400 °C [32]).

Deposition–precipitation (DP) of Au nanoparticles. 0.5 g of hexagonal or monoclinic WO$_3$ was suspended in 150 ml of $3.1*10^{-4}$ M chloroauric acid (HAuCl$_4$) solution. The reaction mixture was stirred for 1 h; then 4 M NH$_4$OH was added to maintain pH 7 in the whole process. After 75 min the reaction was completed, and the liquid phase became colorless. The as-prepared catalysts were washed with de-ionized water and centrifuged three times at room temperature. Consecutively, the catalysts were dried overnight at 60 °C. Prior to the CO oxidation test reactions, the catalysts were pretreated at 350 °C for 1 h in air atmosphere (50 ml min^{-1} flow rate), so that the gold-amine complexes could be completely decomposed and gold nanoparticles could be formed.

Catalyst characterization

Transmission electron microscope (TEM) images about the WO$_3$/Au samples were recorded on a FEI Morgagni 268b instrument operated at 100 keV. At least 200 nanoparticles were measured on the TEM images to define the particle size distribution.

Scanning electron microscopy (SEM) characterization was performed by a LEO-1550 FEG SEM instrument.

Surface area values were deduced from low temperature nitrogen adsorption data (Quantachrome NOVA 2000E) according to the multi point BET model [33].

Powder X-ray diffraction (XRD) patterns were measured by a PANalytical X'pert Pro MPD X-ray diffractometer using Cu K$_\alpha$ radiation.

X-ray Photoelectron (XPS) spectra from the surface of the samples were recorded by a VG Microtech instrument using Mg K$_\alpha$ radiation. The spectrometer was calibrated with the binding energy of the C1s line (285 eV).

Temperature programmed oxidation of CO

Temperature programmed oxidation (TPO) of CO was measured in the temperature range from −30 to 270 °C with a heating rate of 5 °C min^{-1} in a U-tube quartz reactor. 25mg of each catalyst was mixed with 125 mg Al$_2$O$_3$ in order to make a catalyst bed to facilitate formation of plug like flow, and to inhibit the catalysts to occlude the filter. Prior to the CO oxidation reaction, the catalyst samples were pretreated at 350 °C for 1 h in air atmosphere (50 ml min^{-1} flow rate) to generate catalytically active gold nanoparticles on the catalyst supports. Upon completion of the pretreatment, the samples were cooled in helium gas flow. When temperature reached -30 °C, helium flow was replaced with the flow of the gaseous reaction mixture (70 ml min^{-1}), in which the volume ratios were 1.5/1.5/67 for CO/O$_2$/He, respectively. The outlet gas flow was monitored by a quadruple mass spectrometer (Prisma QMS 200, Pfeiffer Vacuum Technology) recording the $m/z = 28^+$, 32^+, and 44^+ signals of consumed CO and O$_2$ and as-formed CO$_2$, respectively.

Results and discussion

Structure, morphology and composition

According to our previous studies, deposition–precipitation method with $HAuCl_4$ and NH_3 solution results gold-amine complexes directly bonded to a metal oxide catalyst support such as SiO_2 or Al_2O_3. In the present work, conditions of catalyst preparations on WO_3 support were similar to that used previously at the Au/SiO_2 and Au/Al_2O_3 catalysts [22-23]. In the case of WO_3 supports, it was noticed that small portion of the complexes started to degrade during the deposition–precipitation process, resulting in sub 5 nm nanoparticles (observed on TEM images not shown here). However, the dominant part of the Au nanoparticles was obtained, only when the amine complexes degraded in air flow during the pretreatment process at 350 °C.

Based on SEM (Fig. 1) and TEM (Fig. 2) images, the estimated size of the h- and m-WO_3 support particles were 50-70 nm and 60-90 nm, respectively. The surface area values (S_{BET}) were 11 and 6.5 m^2/g for pure h- and m-WO_3 particles, respectively.

After the pretreatment process, SEM (Fig. 1) and TEM (Fig. 2) showed that large portion of Au nanoparticles was under the critical 5 nm (Fig. 3), which is required to generate catalytic activity [34]. The supports influenced the Au particle size, as in the case of h-WO_3 43 % of Au particles was under 5 nm, while in the case of m-WO_3 this value was 37 %.

According to XRD patterns (Fig. 4), the supports were pure h-WO_3 (ICDD 85-2460) and m-WO_3 (ICDD 43-1035). Gold (ICDD 04-0784) was identified at about 38° in the case of both catalyst supports (see insets in Fig. 4). No impurities were detected by XRD on the WO_3/Au samples.

The oxidation states of tungsten, oxygen and gold atoms were investigated by XPS (Fig. 5). Though XPS is a surface analytical method with an average information depth of 10 nm, it gave a good estimate also about the bulk composition of the particles. The particle size of our samples was between 50-90 nm. If 70 nm is taken as an average particle size and spherical particles with 35 nm average particle radius are assumed, then XPS can give

7

information about the outer 10 nm shell of the particles. The volume of the outer 10 nm shell is ca. the half (49 %) of the volume of the whole particle. Thus the XPS signal came from half of the complete volume of the particles, which provided a good estimate of the bulk composition of the nanoparticles.

Recently it was shown that while m-WO_3 is completely oxidized, the structure of h-WO_3 is partially reduced. This was explained by that stabilizing cations (Na^+, K^+, NH_4^+, etc) (or water molecules) were always present in the hexagonal channels of h-WO_3, and they stabilized the metastable hexagonal framework [27]. Due to the presence of W^{5+} and W^{4+} atoms, there were less surface OH groups and water molecules on the surface of h-WO_3, compared to m-WO_3 [31].

The different oxidation states of tungsten were confirmed by XPS in the case of the h- and m-WO_3 supports of Au nanoparticles as well. In the m-WO_3/Au catalyst, the m-WO_3 support was basically completely oxidized with 96.7 % W^{6+} atoms detected ($W4f_{7/2}$ peak: 37.3 eV; $W4f_{5/2}$ peak: 35.1 eV). The small amount of W^{5+} atoms (3.3 %; $W4f_{7/2}$ peak: 36.2 eV; $W4f_{5/2}$ peak: 33.6 eV) is due to that m-WO_3 usually obtains a greenish color in the high vacuum of the XPS chamber and its surface gets slightly reduced. However, in as-prepared form, m-WO_3 is completely oxidized. In the h-WO_3/Au catalyst, the h-WO_3 support contained also W^{4+} atoms besides W^{6+} and W^{5+} species (93.6 %, 5%, 1.5%; $W4f_{7/2}$ peaks: 37.2, 36.2, 35.2 eV; $W4f_{5/2}$ peaks: 35.1, 33.6, 32.9 eV for W^{6+}, W^{5+}, W^{4+}, respectively).

The amount of surface O^{2-}, OH^- and H_2O species (530.9, 531.6, 533.5 eV, respectively) was also examined by XPS. Their normalized ratios showed that the amount of surface OH^- was ca. 25 % larger on m-WO_3/Au (1.00/0.69/0.11 for O^{2-}/OH^-/H_2O respectively), compared to h-WO_3/Au (1.00/0.55/0.10 for O^{2-}/OH^-/H_2O respectively). It can be noted that H_2O was present on the surface of h-WO_3 both in physically adsorbed and chemically bonded forms [35], and XPS measures their overall amount.

According to XPS, gold was present only in metallic form (Au4f$_{7/2}$ peak: 83.5 eV; Au4f$_{5/2}$ peak: 87.2 eV) [36-38]. The gold loading of the WO$_3$ supports was different, i.e. 5.3 mass% Au was present on m-WO$_3$, while only 3.7 mass% on h-WO$_3$. The support h-WO$_3$ had larger specific surface, which might result in larger gold loading; however, the opposite was observed. Thus, the larger amount of Au on the m-WO$_3$ support can be explained only by that the amount of surface OH groups was larger on m-WO$_3$, compared to h-WO$_3$. The larger OH density over m-WO$_3$ probably meant more reaction and then nucleation sites for Au reduction and Au nanoparticle formation.

Temperature programmed oxidation of CO

The TPO test results of h-WO$_3$/Au and m-WO$_3$/Au catalysts are presented in Fig 6. Below 100 °C both catalysts exhibited minor activity. In this temperature region (between -30 and 100 °C) the hexagonal support seemed to be better for catalytic activity. There was a minimum in the catalytic activity of both catalysts around 100 °C. From 100 °C the conversion of CO started to increase again in the case of both catalysts, and from this point the activity of m-WO$_3$/Au superseded increasingly that of Au/h-WO$_3$. The activity of both catalysts rose especially dramatically after 150 °C.

On the one hand, due to larger specific surface and larger portion of loaded Au nanoparticles below 5 nm h-WO$_3$ was expected to be a better catalyst support. On the other hand, the larger amount of Au nanoparticles might be an advantage for using the m-WO$_3$ support. According to the catalysis tests, Au/m-WO$_3$ had significantly larger activity above 100 °C, which means that the 43 % larger Au load of the m-WO$_3$ support was the decisive on the catalytic activity, and its influence surpassed the effect of the larger specific surface of h-WO$_3$ and larger portion of Au nanoparticles below 5 nm.

Recently, it was revealed that the higher surface OH density of m-WO_3 was responsible for that it was a better photocatalyst than h-WO_3 [31]. In the present study, the larger amount of surface OH groups on m-WO_3 resulted in larger Au nanoparticle loading on m-WO_3 and better activity of the m-WO_3/Au catalyst, compared to the h-WO_3/Au composite. Thus, though not directly as in photocatalysis, but in an indirect way the higher surface OH density of m-WO_3 was responsible for that m-WO_3 was a better support for the catalytic Au nanoparticles, compared to h-WO_3.

The conversion reached with the Au/m-WO_3 catalyst in CO oxidation is not outstanding compared to previous supported Au catalysts [9-11,20], mostly due to the relatively low specific surface of the m-WO_3 support. However, the aim of the present study was not to prepare the best catalyst for CO oxidation, but to study how the crystal structure of the WO_3 support influences the activity of Au/WO_3 catalysts.

Conclusion

In this work Au/WO_3 catalysts with different WO_3 support crystal forms (hexagonal or monoclinic) were investigated. Au nanoparticles with diameters partially smaller than 5 nm were prepared on WO_3 substrates for the first time with the deposition and precipitation method using $HAuCl_4$ and NH_4OH solutions, followed by a pretreatment in air at 350 °C. Previously it was considered not possible to deposit Au nanoparticles with this method on an oxide with low isoelectronic point (i.e. WO_3). The as-prepared Au/h-WO_3 and Au/m-WO_3 catalysts were characterized with TEM, SEM, N_2-BET specific surface measurement, XRD and XPS.

To reveal the effect of support crystal structure, the catalysts were tested in the oxidation reaction of CO. The catalyst m-WO_3/Au showed considerably larger catalytic

activity over 100 °C compared to h-WO_3/Au. The reason for this is that m-WO_3 is completely oxidized and its surface is rich in OH groups, which are beneficial for Au nanoparticle nucleation. In contrast, h-WO_3 is partially reduced due to stabilizing cation impurities in its structure, resulting in lower surface OH coverage, and thus lower Au nanoparticle loading and lower catalytic activity. This means that m-WO_3 is a better support for catalytic Au nanoparticles.

Acknowledgements

References

[1]   Thompson D (1998) Gold Bull 31:111.

[2]   Haruta M (1997) Catal Today 36:153.

[3]   Pilasombat R, Daly H, Goguet A, Breen JP, Burch R, C. Hardacre, Thompsett D, (2012) Catal Today 180:131.

[4]   Wang L, He L, Liu Y, Cao Y, He H, Fan K, Zhuang J (2009) J Catal 264:145.

[5]   Choudhary V, Dumbre D (2011) Catal Commun 13:82.

[6]   Ahn HG, Choi BM, Lee DJ (2006) J Nanosci Nanotechnol 11:3599.

[7]   Baatz C, Prüße U (2007) Catal Today 122:325.

[8]   Laguna OH, Centeno MA, Romero-Sarria F, Odriozola JA (2011) Catal Today 172:118.

[9]   Ma Z, Dai S (2011) Nano Res 4:3.

[10]   Wenqiang M, Fuyi C (2013) Catal Lett 143:84.

[11]   Haruta M (2014) Angew Chem Int Ed 3:52.

[12]   Bourgeois D (2009) Structure 17:1427.

[13]   Hoffmann MR, Martin ST, Choi W, Bahnemannt DW (1995) Chem Rev 95:69.

[14]   Roos M, Böcking D, Gyimah KO, Kucerova G, Bansmann J, Biskupek J, Kaiser U,
       Hüsing N, Behm RJ (2011) Beilstein J Nanotechnol 2:593.

[15]   Li W, Wang A, Yang X, Huang Y, Zhang T (2012) Chem Commun 48:9183

[16]   Fu Q, Weber A, Flytzani-Stephanopoulos M (2001) Catal Lett 77:87.

[17]   Koo DH, Kim M, Chang S (2005) Org Lett 7:5015.

[18]   Oka K, Nishiguchi T, Kanai H, Utani K, Imamura S (2006) Appl Catal A 309:187.

[19]   Lesnyak VV, Ishchenko EV, Gut IN, Yatsimirskii AV, Boldyreva OY (2007) Russ J
       Phys Chem A 81:874.

[20]   Veith GM, Lupini AR, Pennycook SJ, Villa A, Prati L, Dudney NJ (2007) Catal Today
       122:248.

[21]   Haruta M (2004) J New Mater Electrochem System 7:163.

[22]   Somodi F, Borbáth I, Hegedűs M, Tompos A, Sajó IE, Szegedi Á, Rojas S, Fierro JLG,
       Margitfalvi JL, (2008) Appl Catal A 347:216.

[23]   Somodi F, Borbáth I, Hegedűs M, Lázár K, Sajó IE, Geszti O, Rojas S, Fierro JLG,
       Margitfalvi JL, (2009) Appl Surf Sci 256:726.

[24]   E. Lassner, W.D. Schubert, Tungsten. Properties, Chemistry, Technology of the
       Element, Alloys, and Chemical Compounds (Kluwer Academic/Plenum Publishers,
       New York, 1999).

[25] Szilágyi IM, Saukko S, Mizsei J, Tóth AL, Madarász J, Pokol G (2010) Solid State Sci 12:1857.

[26] Szilágyi IM, Wang L, Gouma PI, Balázsi C, Madarász J, Pokol G (2009) Mater Res Bull 44:505.

[27] Szilágyi IM, Madarász J, Pokol G, Király P, Tárkányi G, Saukko S, Mizsei J, Tóth AL, Szabó A, Varga-Josepovits K (2008) Chem Mater 20:4116.

[28] Balázsi C, Wang L, Zayim EO, Szilágyi IM, Sedlackova K, Pfeifer J, Tóth AL, Gouma PI (2008) J Eur Ceram Soc 28:913.

[29] Szilágyi IM, Saukko S, Mizsei J, Király P, Tárkányi G, Tóth AL, Szabó A, Varga-Josepovits K, Madarász J, Pokol G (2008) Mater Sci Forum 589:161.

[30] Wang L, Pfeifer J, Balázsi C, Szilágyi IM, Gouma PI (2007) Proc SPIE 6769:67690E.

[31] Szilágyi IM, Fórizs B, Rosseler O, Szegedi Á, Németh P, Király P, Tárkányi G, Vajna B, Varga–Josepovits K, László K, Tóth AL, Baranyai P, Leskelä M (2012) J Catal 294: 119.

[32] Szilágyi IM, Hange F, J. Madarász J, Pokol G (2006) Eur J Inorg Chem 17:3413.

[33] Brunauer S, Emmett P, Teller E (1938) J Am Chem Soc 60:309.

[34] G. C. Bond, C. Louis, D.T. Thompson, Catalysis by gold (Imperial College Press, London, 2006).

[35] Szilágyi IM, Pfeifer J, Balázsi C, Tóth AL, Varga-Josepovits K, Madarász J, Pokol G (2008) J Therm Anal Calorim 94:499.

[36] Bogdanchikova N, Pestryakov A, Tuzovskaya I, Zepeda TA, Farias MH, Tiznado H, Martynyuk O (2013) Fuel 110:40.

[37] Ning L, Zhang W, Yan H, Pang H, Ma H, Yu Y (2013) J Coll Interfac Sci 403:91.

[38] Xu J, Huang J, Liu YM, Cao Y, Li YX, Fan KN (2011) Catal Lett 141:198.

Figures
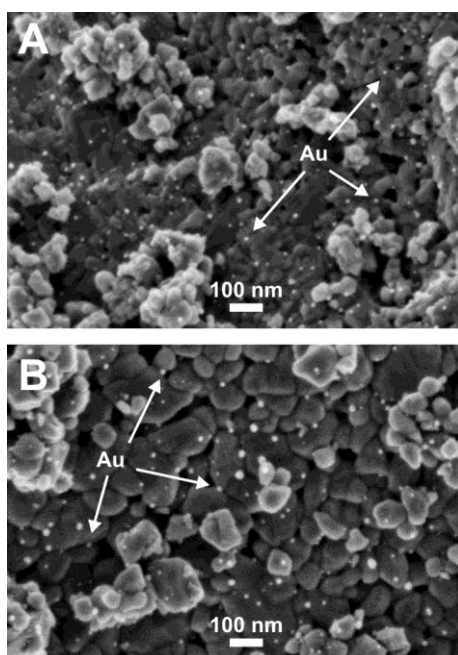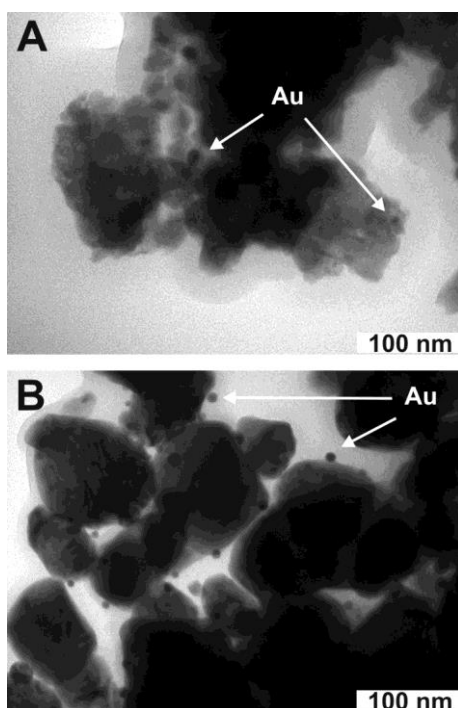

Fig. 1. SEM images of (a) h-WO$_3$/Au and (b) m-WO$_3$/Au
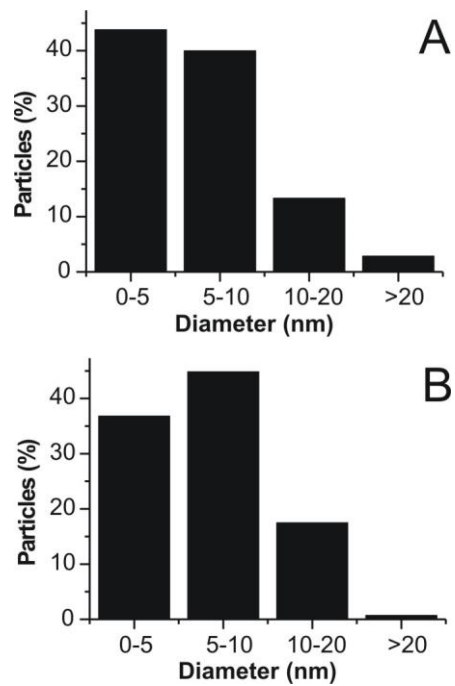

Fig. 2. TEM images of (a) h-WO$_3$/Au and (b) m-WO$_3$/Au

Fig. 3. Size distribution of gold nanoparticles on (a) h-WO$_3$ and (b) m-WO$_3$ supports
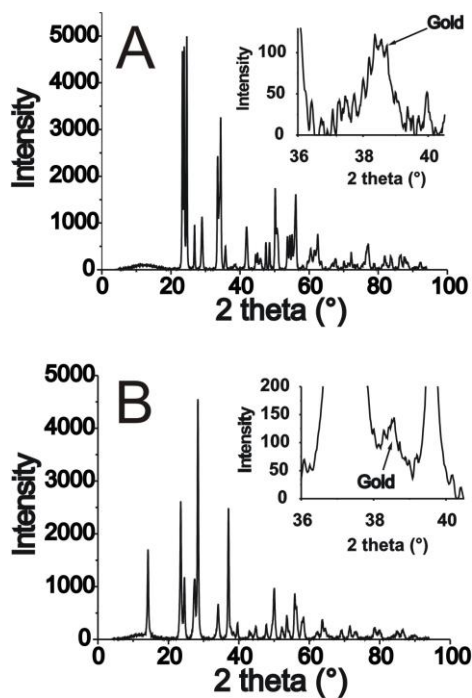

Fig. 4. XRD patterns of (a) h-WO$_3$/Au and (b) m-WO$_3$/Au. The insets show the presence of
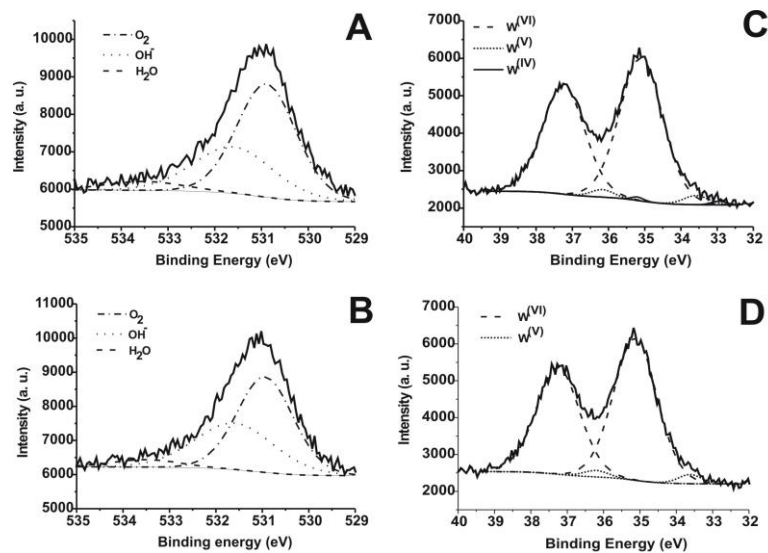
gold on the surface of the WO$_3$ supports.

Fig. 5. XPS spectra of (a) O1s region of h-WO$_3$/Au; (b) O1s region of m-WO$_3$/Au; (c)
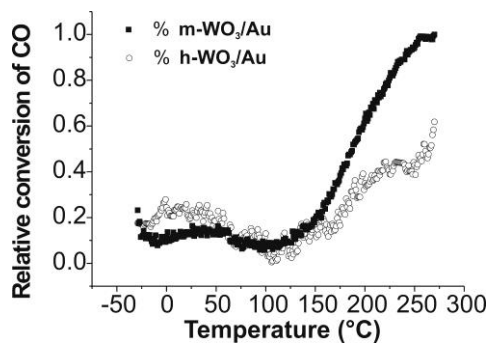
W4f region of h-WO$_3$/Au; (a) W4f region of m-WO$_3$/Au

Fig. 6. Activity of h-WO$_3$/Au and m-WO$_3$/Au catalysts in CO oxidation